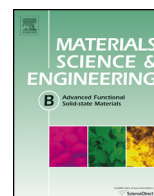




Contents lists available at ScienceDirect

# Materials Science and Engineering B

journal homepage: [www.elsevier.com/locate/mseb](http://www.elsevier.com/locate/mseb)



## High energy density layered-spinel hybrid cathodes for lithium ion rechargeable batteries

S. Basu<sup>a,\*</sup>, P.P. Dahiya<sup>b</sup>, Mainul Akhtar<sup>b</sup>, S.K. Ray<sup>a</sup>, J.K. Chang<sup>c</sup>, S.B. Majumder<sup>b</sup>

<sup>a</sup> Department of Physics, Indian Institute of Technology Kharagpur, Kharagpur 721 302, India

<sup>b</sup> Materials Science Center, Indian Institute of Technology Kharagpur, Kharagpur 721 302, India

<sup>c</sup> Institute of Materials Science and Engineering, National Central University, Taiwan

### ARTICLE INFO

#### Article history:

Received 15 February 2016

Received in revised form 29 March 2016

Accepted 12 April 2016

Available online xxx

### ABSTRACT

High energy density  $\text{Li}_2\text{MnO}_3$  (layered)– $\text{LiMn}_{1.5}\text{Ni}_{0.5}\text{O}_4$  (spinel) composite cathodes have been synthesized using auto-combustion route. Rietveld refinements together with the analyses of high resolution transmission electron micrographs confirm the structural integration of  $\text{Li}_2\text{MnO}_3$  nano-domains into the  $\text{LiMn}_{1.5}\text{Ni}_{0.5}\text{O}_4$  matrix of the composite cathodes. The discharge capacity of the composite cathodes are due to the intercalation of  $\text{Li}^+$  ion in the tetrahedral (8a) and octahedral (16c) sites of the spinel component and also the insertion of  $\text{Li}^+$  in the freshly prepared  $\text{MnO}_2$  lattice, formed after  $\text{Li}_2\text{O}$  extraction from the  $\text{Li}_2\text{MnO}_3$  domains. The capacity fading of the composite cathodes are explained to be due to the layered to spinel transition of the  $\text{Li}_2\text{MnO}_3$  component and  $\text{Li}^+$  insertion into the octahedral site of the spinel lattices which trigger cubic to tetragonal phase transition resulting volume expansion which eventually retard the  $\text{Li}^+$  intercalation with cycling.

© 2016 Elsevier B.V. All rights reserved.

### 1. Introduction

To develop high energy density batteries for electric vehicles (EV) extensive research is being performed to identify novel cathode materials which will be effective alternative to the current layered, spinel and olivine based cathodes used in existing lithium ion batteries for consumer electronics. Through various research reports it has been understood that the electrochemical activation (by charging it beyond 4.5 V) of  $x\text{Li}_2\text{MnO}_3 - (1-x)\text{LiMO}_2$  ( $M = \text{Mn, Ni, Co}$ ) composite cathode leads to oxide materials that deliver high initial capacities ( $\sim 250 \text{ mAh g}^{-1}$ ) [1–6]. These composite cathodes are also termed as lithium manganese rich (LMR) layered oxides and alternatively represented as  $\text{Li}(\text{Li, Mn, Ni, Co})\text{O}_2$ , where Li is also present in the transition metal oxide layer. Though these LMR cathodes exhibit significantly higher capacities, they are plagued with low first cycle Coulombic efficiency, poor rate capabilities, and appreciable voltage decay during repeated charge–discharge cycling [7–9]. Despite the variation of space group symmetries, structural integration and electrochemical characteristics of layered  $\text{Li}_2\text{MnO}_3$  (SG  $C2/m$ , monoclinic) and spinel  $\text{LiMn}_{1.5}\text{Ni}_{0.5}\text{O}_4$  ( $Fd-3m$ , cubic) has recently been demonstrated. Additionally, the electrochemical

characteristics of layered–layered composite with spinel has also been reported [10–19]. As a spinel component, ordered  $\text{LiMn}_{1.5}\text{Ni}_{0.5}\text{O}_4$  is fundamentally different from  $\text{LiMn}_2\text{O}_4$  spinel, as in the former Mn ions remain predominantly in +4 valence state and the redox activity of Ni cations ( $\sim 4.7 \text{ V}$ ) is primarily due to the intercalation of  $\text{Li}^+$  ions in the tetrahedral 8a site of the spinel lattice. This limits the discharge capacity of  $\text{LiMn}_{1.5}\text{Ni}_{0.5}\text{O}_4$  spinel  $\sim 147 \text{ mAh g}^{-1}$ . Theoretically,  $\text{Li}^+$  ions can also be inserted in 16c octahedral site of the spinel lattice  $\sim 2.8 \text{ V}$  resulting the reduction of  $\text{Mn}^{4+}$  ions to  $\text{Mn}^{3+}$  yielding theoretical discharge capacity  $\sim 294 \text{ mAh g}^{-1}$  [20,21]. However, the insertion of  $\text{Li}^+$  ions in the octahedral sites triggers cubic to tetragonal structural phase transition (Jahn–Teller distortion) which is associated with about 5% volume change [22]. The phase transition induced strain is believed to be too large for maintaining structural integrity of the spinel cathode with the current collector and eventually retards the Li ion insertion with repeated cycling resulting capacity fading.

The aim of the present work is to investigate if, by structurally integrating layered  $\text{Li}_2\text{MnO}_3$  component into the  $\text{LiMn}_{1.5}\text{Ni}_{0.5}\text{O}_4$  matrix, one can yield composite cathodes with discharge capacities significantly higher than the individual layered and spinel component. The three dimensional interstitial space of the spinel component is expected to ensure high rate capability of the composite cathodes. Also it would be interesting to investigate if the integration of the layered component has any effect to retard the Jahn–Teller distortion which results due to the

\* Corresponding author. Tel.: +91 9933977529; fax: +91 3222282700.  
E-mail address: [sbasumajumder@yahoo.com](mailto:sbasumajumder@yahoo.com) (S. Basu).

insertion of  $\text{Li}^+$  into the octahedral sites of the spinel lattice. In view to this, in the present work we have synthesized a series of  $x\text{Li}_2\text{MnO}_3 - (1-x)\text{LiMn}_{1.5}\text{Ni}_{0.5}\text{O}_4$  ( $x=0, 0.1, 0.3, 0.5$  and  $1.0$ ) composite cathodes by auto-combustion synthesis. The nature of structural integration of the layered and spinel components have been investigated by X-ray diffraction in conjunction with high resolution transmission electron microscopy. The electrochemical characteristics of the synthesized cathodes have been investigated by cyclic voltammetry, charge–discharge, cycleability and rate capability characteristics in the voltage window between 2.5 and 4.8 V, using current rate in the range of 10–100  $\text{mA g}^{-1}$ .

## 2. Experimental

In the present work we have synthesized  $x\text{Li}_2\text{MnO}_3 - (1-x)\text{LiMn}_{1.5}\text{Ni}_{0.5}\text{O}_4$  ( $x=0, 0.1, 0.3, 0.5$  and  $1.0$ ) cathode powders using auto-combustion synthesis. Stoichiometric amount of lithium acetate, manganese acetate and nickel acetate were used as precursor materials without further purification. For example, for  $x=0.5$  composite, lithium acetate, manganese acetate and nickel acetate were taken in the ratio of 6:5:1. The salts were dissolved separately in warm distilled water (at  $60^\circ\text{C}$ ) through continuous stirring. These salt solutions were mixed together through continuous stirring and few ml of 70%  $\text{HNO}_3$  solution was added into it to avoid any precipitation. Aqueous citric acid and ethylene glycol solution (1:3 molar ratio) was added to the mixed precursor maintaining the citrate to metal ion ratio  $\sim 1:1$ . We have found that upon vigorous stirring and simultaneous heating at  $\sim 120^\circ\text{C}$  the solution transformed into a gel. The gel was auto ignited to form fluffy black powder. The dried powder was hand ground in a mortar-pestle and calcined at  $450^\circ\text{C}$  for 3 h in air. The calcined powder was pressed into the form of circular pellets and these pellets were calcined at  $800^\circ\text{C}$  for 8 h for crystallization.

The calcined pellets were crushed into powders and the phase formation behaviour of the calcined powder was characterized using an X-ray diffractometer (Bruker, D8 Advance). X-ray diffractograms of the cathode powders were recorded at a scanning speed of  $1.2\text{ min}^{-1}$  in a  $2\theta$  range of  $10\text{--}75^\circ$  using  $\text{Cu K}\alpha$  radiation. The diffraction data were refined by Rietveld method using MAUD software [23]. The surface morphology of the synthesized cathode powders were characterized using a field-emission scanning electron microscope (SUPRA-40, Carl Zeiss SMT, Germany). The high-resolution transmission electron micrographs (HRTEM) of the cathode particles are characterized using a transmission electron microscope (JEM 2100, JEOL Ltd., Japan).

The electrochemical characteristics of the synthesized cathode powders were investigated by fabricating CR2032 type coin cells. To fabricate the cathode composite, a slurry was made by mixing cathode powders with acetylene black (as conducting agent) and polyvinylidene fluoride (PVDF) (as binder) (in a weight ratio of 80:10:10 respectively) in N-methyl-2-pyrrolidone (NMP) solvent. The slurry was tape cast on aluminium foil to form cathode layer about  $60\text{ }\mu\text{m}$  thick. The tape cast layer was vacuum dried overnight at  $100^\circ\text{C}$ . Circular discs of 15 mm diameter were cut out of the dried cathode layer on aluminium current collector. The average mass loading of cathode powder was about  $3.5\text{ mg/cm}^2$ . Lithium metal foils were used as counter and reference electrodes.  $\text{LiPF}_6$  (1 M) in a 1:1 (by weight) mixture of ethylene carbonate and diethyl carbonate was used as electrolyte. Celgard 2400, soaked with electrolyte was used as separator between anode and cathode. The cathode, separator and anode were crimped together using a crimping machine (MT-190-20, MTI Corporation, USA) inside a moisture and oxygen controlled ( $<1.0\text{ ppm}$ ) glove box (Labstar, Mbraun Inc., Germany) to fabricate CR 2032 type coin cell. Galvanostatic charge–discharge cycling in the voltage range 2.5–4.8 V was

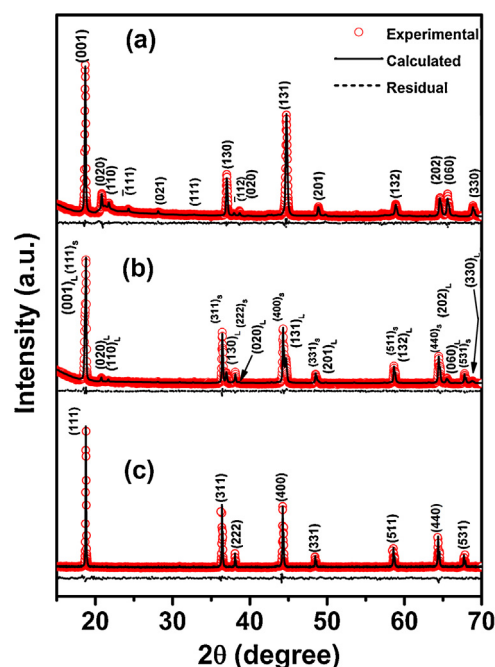


**Fig. 1.** X-ray diffractograms of (a)  $\text{Li}_2\text{MnO}_3$ , (b)  $0.5\text{Li}_2\text{MnO}_3\text{--}0.5\text{LiMn}_{1.5}\text{Ni}_{0.5}\text{O}_4$  and (c)  $\text{LiMn}_{1.5}\text{Ni}_{0.5}\text{O}_4$  calcined powder. The solid lines are the Rietveld refined patterns. The layered ( $\text{Li}_2\text{MnO}_3$ ) and spinel ( $\text{LiMn}_{1.5}\text{Ni}_{0.5}\text{O}_4$ ) diffraction peaks are indexed with subscript 'L' and 'S' in the composite powder.

carried out with an automated battery tester (BST8-MA, MTI Corporation, USA). A potentiostat–galvanostat system (Gamry Inc., USA) and allied electrochemical analysis software (PHE 200) were used for cyclic voltammetry measurement and analysis.

## 3. Results and discussion

### 3.1. Structural and microstructural characteristics

Fig. 1 shows the X-ray diffraction patterns of calcined (a)  $\text{Li}_2\text{MnO}_3$ , (b)  $0.5\text{Li}_2\text{MnO}_3\text{--}0.5\text{LiMn}_{1.5}\text{Ni}_{0.5}\text{O}_4$  and (c)  $\text{LiMn}_{1.5}\text{Ni}_{0.5}\text{O}_4$  powders prepared by auto-combustion synthesis. The experimental X-ray diffractograms of  $\text{Li}_2\text{MnO}_3$  and  $\text{LiMn}_{1.5}\text{Ni}_{0.5}\text{O}_4$  powders were refined (solid lines) assuming monoclinic  $\text{C2/m}$  and cubic  $\text{Fd-}3m$  space group respectively (Fig. 1(a) and (c)). As shown in Fig. 1(b) the  $0.5\text{Li}_2\text{MnO}_3\text{--}0.5\text{LiMn}_{1.5}\text{Ni}_{0.5}\text{O}_4$  composite powder was refined assuming a mixture of both  $\text{C2/m}$  (layered  $\text{Li}_2\text{MnO}_3$ ) and  $\text{Fd-}3m$  (spinel  $\text{LiMn}_{1.5}\text{Ni}_{0.5}\text{O}_4$ ) space groups. The diffraction peaks from the layered (marked L) and spinel (marked S) is clearly indexed in the refined pattern. The refined atomic coordinates and the structural parameters for  $0.5\text{Li}_2\text{MnO}_3\text{--}0.5\text{LiMn}_{1.5}\text{Ni}_{0.5}\text{O}_4$  composite is tabulated in Table 1. Note that the estimated weight fraction agrees quite well with the nominal composition. We have performed X-ray Rietveld refinement for other synthesized composite cathodes and the refined lattice parameters, crystallite size and weight fraction of layered and spinel phases are tabulated in Table 2. It is interesting to note that the lattice parameters of the constituent layered and spinel phases are marginally changed in all the composite cathode compositions. This indicates nominal cation/(s) diffusion between the constituent phases in all the composite powders.

Fig. 2 shows the surface morphologies of calcined (a)  $\text{Li}_2\text{MnO}_3$ , (b)  $0.5\text{Li}_2\text{MnO}_3\text{--}0.5\text{LiMn}_{1.5}\text{Ni}_{0.5}\text{O}_4$  composite and (c)  $\text{LiMn}_{1.5}\text{Ni}_{0.5}\text{O}_4$  powders prepared by auto-combustion synthesis. As envisaged in these micrographs,  $\text{Li}_2\text{MnO}_3$  has comparatively larger particle size as compared to  $\text{LiMn}_{1.5}\text{Ni}_{0.5}\text{O}_4$  particles. As outlined in Section 2, we have synthesized layered–spinel composite powders by the auto-combustion of molecularly mixed layered

Download English Version:

<https://daneshyari.com/en/article/5448790>

Download Persian Version:

<https://daneshyari.com/article/5448790>

[Daneshyari.com](https://daneshyari.com)